Carbohydrate Research, 189 (1989) 31–48
Elsevier Science Publishers B.V., Amsterdam – Printed in The Netherlands

CRYSTALLIZATION BEHAVIOR OF AMYLOSE-V COMPLEXES: STRUCTURE–PROPERTY RELATIONSHIPS

COSTAS G. BILIADERIS AND GRANT GALLOWAY
Dept. of Food Science, University of Manitoba, Winnipeg, Manitoba R3T 2N2 (Canada)
(Received August 2nd, 1988; accepted for publication December 22nd, 1988)

ABSTRACT

The effect of temperature on the crystallization behavior of amylose–lipid complexes from dilute solution has been investigated by differential scanning calorimetry, X-ray diffraction, and structural analysis using alpha amylase etching–gel permeation chromatography, as well as birefringence, density, and dynamic rheological measurements. For any given monoglyceride used as a complexing ligand (monomyristin, monopalmitin, or monostearin), two thermally distinct forms of the complex were identified, namely, I (low T_m) and II (high T_m), depending on the crystallization temperature (T_c); complex I predominated at low T_c, while II was the preferred form at high T_c. Minor differences between the two forms in the size distribution of chain segments constituting the ordered regions are inadequate to explain the lack of a well defined V-pattern for form I. Instead, explanations of a number of thermal and physicochemical properties can be provided if it is postulated that form I is a separate thermodynamic state, with internal energy and entropy intermediate between those of a melt and of a classical crystalline system, such as form II. Form I is assumed to be formed when rapid nucleation occurs, and is morphologically described by a random distribution of the basic structural elements (*i.e.* helical segments), having little crystallographic register. A prerequisite for the conversion I→II is the partial melting of its structure, which appears to foster crystallite formation and thickening by chain diffusion. Annealing effects on form II of the crystals of V were also found typical of metastable semicrystalline polymers.

INTRODUCTION

Amylose forms crystalline complexes with a number of polar and non-polar compounds which, when characterized crystallographically, were found to exhibit the well defined V-amylose structure. Early X-ray diffraction studies indicated that the polysaccharide assumes a helical conformation, and that the diameter of the helix is controlled by the size of the complexing agent. Evidence has been presented indicating that linear alcohols and fatty acids form helices having 6 D-glucosyl

0008-6215/89/$ 03.50

residues per turn[1-5], branched-chain alkyl compounds (*e.g. tert*-butyl alcohol) form helices of 7 D-glucosyl residues per turn[5-8], and other bulkier molecules (*e.g.*, 1-naphthol) yield helices of 8 D-glucosyl residues per turn[9]. Electron and X-ray diffraction data[3,4,10], as well as digestion with alpha amylase followed by gel-permeation chromatography of the resistant amylodextrin fragments[11], suggest a lamella-like organization of amylose V-complexes; *i.e.*, the polysaccharide chains are so folded as to have their chain axes perpendicular to the surface of the lamella. The long spacings calculated by the Bragg equation indicated[3,4] lamella thicknesses lying between 75 and 100 Å. The enzyme structural analysis data of Jane and Robyt[11] also suggested a repeating fold-length of ~100 Å. However, despite the acknowledged helical-chain conformation, a complete characterization of the supermolecular structure and its relationship with the properties of these complexes is a difficult task because they can exist in various states of aggregation.

Attempts to characterize the thermal behavior of amylose–lipid complexes in aqueous environments have recently been made by using differential scanning calorimetry[12-18] (d.s.c.). In a previous series of reports[17-20], we identified the moisture content and the type of ligand as critical parameters controlling the order→disorder processes of aqueous starch and amylose-V complexes. These studies indicated that the thermal profiles of these systems often reflect non-equilibrium melting phenomena (*i.e.*, melting with reorganization) of various metastable states, particularly at intermediate water contents[17-22] (<70% w/w).

With regard to thermal crystallization of polymers, it is known that the melting temperature (T_m) increases with an increase in the crystallization temperature (T_c), and that T_m of lamellar crystals, measured under zero-entropy-production conditions (*i.e.*, melting without reorganization), is directly linked to lamellar thickness[23]. In this respect, and according to classical nucleation theories[23], crystallite thicknesses are inversely proportional to supercooling, $\Delta T = T_m - T_c$. Such relationships can provide direct structural information of metastable crystalline systems by using thermal analysis data. However, very little is known about the temperature-dependence of crystal size and morphology for V-amylose[11]. The present study was, therefore, undertaken in order to gain a better understanding of the role of temperature and ligand on the crystallization mode of V-amylose obtained from dilute solutions. Furthermore, this investigation aimed to provide some insight into the supermolecular organization and property–structure relationships of these polycrystalline materials.

EXPERIMENTAL

Materials. — Lysolecithin from egg yolk, monomyristin (1-C14), monopalmitin (1-C16), and monostearin (1-C18) were products of Sigma Chemical Company (St. Louis, Mo). Potato amylose was obtained from Aldrich Chemical Company (Milwaukee, WI). The molecular characteristics of this polysaccharide were: $[\eta]$ in M KOH = 156 mL.g^{-1}, corresponding[24] to a $\overline{d.p.}$ of 1150 ($\overline{d.p.} = 7.4\ [\eta]$),

iodine affinity = 18.9 g of I_2/100 g, β-amylolysis = 83.8 ±1.1%, and λ_{max} of amylose–iodine complex = 620 nm. Gel-filtration chromatography of this material on a column (2.6 × 90 cm) of Sephacryl S-1000 (superfine) eluted at a flow rate of 0.4 mL.min^{-1} with 2:3 (v/v) dimethyl sulfoxide (Me_2SO)–distilled water revealed a broad bell-shape distribution of the chains. Alpha-amylase preparations from *Bacillus subtilis* (BSA) and hog pancreas (PPA) in ammonium sulfate (3.2M, pH 6.0) were obtained from Boehringer Mannheim Canada, Ltd. (Dorval, Que.). A glucoamylase preparation from *Aspergillus niger,* Diazyme L-200, was provided by Miles Laboratories (Elkhart, IN), and isoamylase from *Pseudomonas amyloderamosa* was a product of Sigma Chemical Company. D-Glucose in enzymic hydrolyzates of α-D-glucans was determined by the D-glucose oxidase–peroxidase method, using a Glucose Diagnostic Kit supplied by Sigma.

Enzyme activities. — Enzyme activities of the α-amylase preparations were assayed by the method of Jane and Robyt[11]. One unit of activity is defined as the amount of enzyme needed to liberate reducing sugars (according to Nelson's test[25]) equivalent to 1 μmol of D-glucose per min from a 0.5% (w/v) aqueous solution of soluble starch (Fisher Scientific, Ottawa, Ont.) under optimum conditions (3mM NaCl in 50mM phosphate buffer, pH 5.5 or 6.9 for BSA or PPA, respectively).

Preparation of amylose-V complexes. — Amylose (400 mg) was hydrated with distilled water (1 mL) and then dissolved[17] in hot Me_2SO (10 mL). The clear solution was diluted with hot water at 95° to a final concentration of 0.25% (w/v). Amylose solutions were equilibrated at the desired crystallization temperature in a temperature-controlled bath before a methanolic solution of the complexing ligand was added under vigorous stirring[17]. The weight ratio of amylose to the added ligand was[26] 5:1. Complex-formation was carried out for 24 h, and the solutions were then cooled to room temperature and allowed to stand for 48 h. The insoluble complexes were recovered by centrifugation (8,000 × *g*), washed repeatedly with chloroform to remove the free ligand (as assessed by d.s.c. analysis), and freeze-dried. For the amylose–monostearin complexes used for α-amylase digestion and structural analysis, large quantities (400 mg per batch) were prepared while maintaining the same amylose concentration and amylose:ligand ratio.

Enzyme digestion and gel-filtration chromatography. — Amylose–monostearin complexes were digested with α-amylase by using procedures similar to those of Jane and Robyt[11]. Typical digestion conditions involved suspending 300 mg of the complex in 60 mL of buffer (6mM NaCl and 0.02% NaN_3 in 0.1M phosphate buffer, pH 5.5 or 6.9 for BSA or PPA, respectively) in the presence of 15 IU of α-amylase. Digestion was carried out at 25° under gentle agitation. At specified time-intervals (0.5 to ~100 h), aliquots of the supernatant liquors were analyzed for total carbohydrates by enzymic hydrolysis with glucoamylase (30–250 μg of carbohydrate/mL, 1 IU of glucoamylase) and subsequent D-glucose determination by the D-glucose oxidase–peroxidase–*o*-dianisidine method. For D-glucose assay, aliquots (5–100 μg of D-glucose/0.5–2.0 mL) were mixed with 5 mL of the enzyme reagent, and absorbances were measured at 450 nm. The extent of hydrolysis was

determined by expressing the total carbohydrates in the supernatant liquor (amount of D-glucose) as percent of the initial complex.

Amylodextrin residues obtained following α-amylase treatment for 48 h were chosen for subsequent gel-filtration analysis. In preparing these materials for chromatography, α-amylase activity was arrested by the addition of 9 volumes of ethanol, and the residual solids were obtained by centrifugation (8,000 × *g*). The complexed monoglyceride was removed from the undigested residues after solubilization with Me_2SO (15 mL), dilution with distilled water (15 mL), and extraction with 2:1 chloroform–methanol (50 mL). This extraction step was repeated twice and, after precipitation from the aqueous phase with ethanol and washing with the same solvent, the amylodextrin was dried under vacuum. Gel-permeation chromatography of the amylodextrin residues was carried out on a column (2.6 × 90 cm) of Sephacryl S-200 (superfine) at a flow rate of 0.4 mL.min^{-1} at 22° by eluting with 2:3 (v/v) Me_2SO–distilled water. Typical sample-injection volumes were 5 mL. Fractions (5 mL) were collected, and assayed enzymically for total carbohydrate as already described. The column was calibrated by fractionating debranched waxy-corn amylopectin[27] and pooled residual amylodextrins from the 24- and 72-h-digested complexes. In this case, the column was loaded with 80–120 mg of carbohydrate material in order to provide detectable reducing power in the eluted fractions of higher d.p. The $\overline{d.p.}$ of each fraction was thus determined by dividing the total carbohydrate concentration by its reducing capacity[25]. A calibration curve was established between $\overline{d.p.}$ and K_{av}; the latter is defined as the ratio $(V_e - V_o)/(V_t - V_o)$, where V_e is the elution volume, V_o is the void volume, and V_t is the total volume:

$$\ln(\overline{d.p.}) = 5.873 - 3.055\, K_{av},\ n = 34,\ r = 0.98,\ p < 0.001.$$

Rheological measurements. — A Bohlin Rheometer System (Lund, Sweden) was employed to characterize the rheological behavior of 10% (w/v) aqueous suspensions of amylose-V complexes. The dynamic measurements were made by using a cone-plate system (30-mm radius and an angle of 5.4°) at 20°. Oscillatory measurements were performed between 0.1 and 20 Hz at a strain amplitude of 0.02. In small-amplitude oscillatory testing of viscoelastic materials, a sinusoidal strain is applied to the sample; the resultant, sinusoidal stress function is analyzed into its in-phase and out-of-phase components. Storage (G′) and loss (G″) moduli are defined as: G′ = (in-phase stress)/(strain) and G″ = (out-of-phase stress)/(strain). These parameters characterize the dynamic response, and provide information about the structure of viscoelastic materials (G′, solid-like behavior, and G″, viscous character).

X-ray diffraction studies. — Hydrated amylose-V complexes were deposited as 2-mm thick films on aluminum holders, and analyzed with a Philips PW 1710 powder diffractometer equipped with a graphite crystal monochromator. The operating conditions were: copper K_α radiation; voltage, 40 kV; recorder time

constant, 0.5 s; sampling-interval time, 0.4 s; recorder speed, 10 mm/2 θ°; and scan speed, 0.1 × 2 θ°/s.

Turbidity measurements. — The time-dependent changes in turbidity of amylose-V aqueous suspensions (0.4 mg/mL), used as an index of the particle density, were monitored by transmittance readings at 580 nm (25°).

Birefringence measurements. — For birefringence, dilute samples of amylose-V aqueous dispersions were viewed, under fully crossed polarizing filters, with a Zeiss Universal research microscope.

Differential scanning calorimetry. — The d.s.c. studies were carried out using a DuPont 9900 Thermal Analyzer equipped with a DuPont 910 cell base and a pressure d.s.c. cell. The system was calibrated with indium. Pressure of 1400 kPa with N_2 was used for all experiments in order to eliminate the problem of pan failure due to moisture loss at temperatures >120°. All samples were prepared in DuPont coated hermetic pans by adding de-ionized water to a preweighed dry sample of the complex, and allowing water to evaporate until the desired moisture content was achieved. A Dow Corning 340 heat-sink compound (Dow-Corning, Midland, MI) was used in order to improve the thermal contact between the pans and the thermocouple detectors. Data were collected at 0.4-s intervals (heating rate 10°/min), and the melting-transition characteristics (enthalpy, peak temperature) were determined by using the DuPont software analysis programs.

RESULTS

Crystallization of aqueous amylose solutions in the presence of monoglycerides or lysolecithin was conducted isothermally in order that the effect of temperature and ligand type on crystal form might be examined. The d.s.c., birefringence, and X-ray diffraction characteristics of the various complexes are summarized in Table I, and representative thermal curves are shown in Fig. 1 for the amylose–monomyristin samples. The d.s.c. data for all samples described in Table I were gathered by heating the complexes with an excess of water (80% w/w) in order to approach zero-entropy-production melting-conditions[17,18]. Under these conditions, melting is highly cooperative, yielding a single endothermic transition. In contrast, when the water content is lessened, the thermal profiles become indicative of metastable melting[17,18]. Recrystallization, superimposed on melting, leads to complicated secondary thermal events as may be seen from Fig. 2b. The well defined exothermic effect between the two endotherms (I and II) for the amylose–monopalmitin complex (50% w/w) gives a strong indication of structural rearrangements occurring during heating in the d.s. calorimeter. Additional evidence for such behavior was provided[18] in studies of the effects of moisture content and heating rate on the melting properties of these materials. Thus, under dynamic heating of complexes with an excess of water, and at high heating-rates, relative to the recrystallization rate, secondary recrystallization-processes can be minimized and, consequently, the thermal profiles would tend to reflect the

TABLE I

D.S.C., BIREFRINGENCE, AND X-RAY DIFFRACTION CHARACTERISTICS OF AMYLOSE-V COMPLEXES CRYSTALLIZED AT VARIOUS TEMPERATURES FROM DILUTE SOLUTIONS (0.25% w/v)

Complexing ligand	*Crystallization temperature (°C)*	*Tp_1 (°C)*	*ΔH_1 (J/g)*	*Tp_2 (°C)*	*ΔH_2 (J/g)*	*Birefringence*	*X-Ray pattern (hydrated complex)*
Monomyristin	55	90.5 ±1.3[a]	20.0 ±0.8			none	amorphous-like
(1-C14)	60	90.8 ±0.9	19.8 ±1.4			none	amorphous-like
	65	91.0 ±0.4	20.7 ±1.2	113.8 ±0.2	1.3 ±0.3		
	75	90.5 ±0.2	16.7 ±0.9	113.0 ±0.7	4.1 ±1.0		
	80	89.3 ±1.1	11.8 ±0.7	112.6 ±0.9	10.5 ±1.2		
	90	91.3 ±0.8	2.9 ±0.8	112.5 ±1.1	15.6 ±1.5	partial	V
Monopalmitin	55	95.9 ±1.1	17.2 ±1.1				
(1-C16)	60	96.2 ±0.6	18.1 ±0.9			none	amorphous-like
	65	95.1 ±0.8	17.9 ±1.2				
	75	95.9 ±0.6	16.9 ±1.9	114.5 ±0.8	2.8 ±1.3		
	80	94.8 ±0.9	13.8 ±1.4	113.7 ±0.6	6.7 ±2.0		
	90	95.0 ±0.8	1.1 ±0.4	112.9 ±1.0	18.3 ±1.1	partial	V
Monostearin	60	100.1 ±1.2	22.2 ±1.8			none	amorphous-like
(1-C18)	90			114.3 ±0.8	23.1 ±0.9	partial	V
Lysolecithin	55	103.1 ±1.0	21.5 ±1.1				
	60	102.3 ±0.4	22.2 ±1.3				
	65	102.4 ±0.3	22.8 ±0.8				
	75	102.3 ±0.9	22.8 ±0.2				
	80	102.0 ±0.8	23.1 ±1.0				
	90	102.2 ±0.9	20.5 ±1.3				

[a]Mean and standard deviations of three replications.

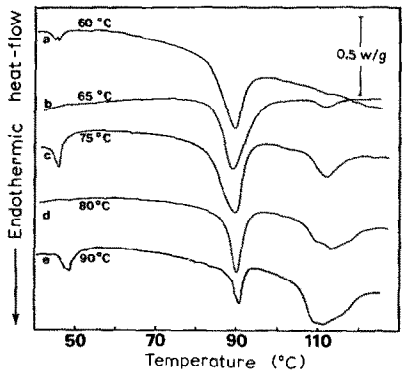

Fig. 1. D.s.c. thermal curves of amylose–monomyristin complexes (20% w/w in H_2O) crystallized at various temperatures (60–90°). Weight of complex, from top to bottom (mg): 2.00, 1.96, 1.70, 1.48, and 1.74.

structural composition of the starting material. The small endothermic transitions at 45–47° (see Fig. 1a, c, and e, and Fig. 2a, b, and c) correspond to the melting of uncomplexed monoglyceride.

Although all amylose–lysolecithin complexes exhibited similar d.s.c. transition-characteristics (see Table I), regardless of the crystallization temperature (T_c), amylose–monoglyceride complexes gave two distinct structural forms (I and II) as shown in Fig. 1 and Table I. These are in accord with previous d.s.c. studies[17,18] and

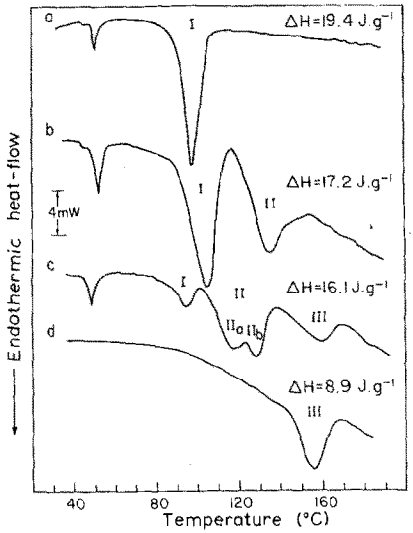

Fig. 2. D.s.c. thermal curves of 60°-crystallized amylose–monopalmitin complex (AM-1C16) and amylose gel. Samples and weight of solids (mg) from top to bottom: (a) AM-1C16, 20% w/w (2.31); (b) AM-1C16, 50% w/w (4.53); (c) re-scan of sample b; and (d) amylose, 50% w/w (5.21). All data files were normalized to a constant weight of solid of 5.00 mg. For definition of symbols, see Table I.

the calorimetric findings of Kowblansky[16] on complexes of amylose with long-chain aliphatic compounds. The transition-peak temperatures, particularly of form I, increase with increasing chain-length of the ligand molecule (see Table I). However, for each monoglyceride, the respective melting temperatures of the complex (forms I and II) remain relatively constant over the broad range of crystallization temperatures examined (55–90°). The data in Table I and the d.s.c. curves in Fig. 1 also show that there is a variation in the transition enthalpies of forms I and II with increasing T_c. As T_c is increased from 55 to 90°, the amount of complex I formed decreases while there is a concomitant development of form II. Interestingly, under conditions where a mixture of both forms is obtained, the sum of ΔH_1 and ΔH_2 is close to the transition enthalpy of the complexes when only one form is present. This constancy in ΔH suggests that both I and II involve the same stabilizing forces and that differences between them are mainly entropic[16]. When crystallized from the "melt" (*i.e.*, at high polymer concentration), an additional melting transition (III) could evolve, as shown in Fig. 2c. This endotherm (thermally reversible) most likely reflects the gel → sol process of uncomplexed amylose-chain segments forming a gel network by molecular entanglement. Indeed, the melting transition of 50% (w/v) aqueous amylose (see Fig. 2d) in the same temperature-region provides additional evidence for such a postulate. The multiple endotherms II_a and II_b are indicative of structural metastability, and so are bound to be rate-dependent, as previously reported[18].

Birefringence measurements and X-ray diffraction analyses were carried out to determine whether the complexes differ in crystallinity. The experimental results indicated that only form II exhibits birefringent properties and has the distinct V-

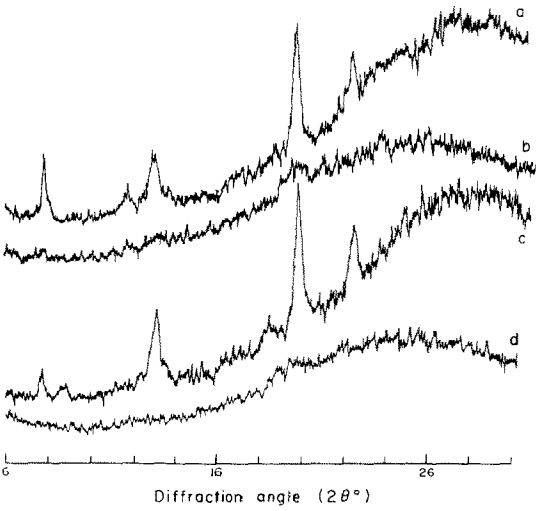

Fig. 3. X-Ray diffraction diagrams of wet amylose–monoglyceride complexes obtained at various crystallization temperatures: (a) 1-C16/90°, (b) 1-C16/60°, (c) 1-C14/90°, and (d) 1-C14/60°. For definition of symbols, see Table I.

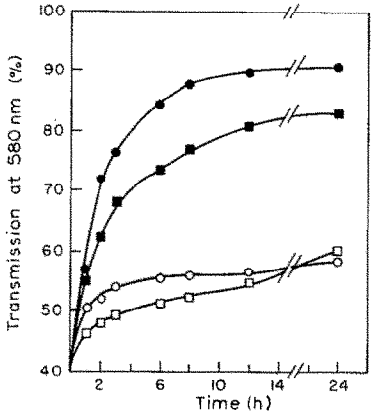

Fig. 4. Time-dependent changes in turbidity of amylose-V aqueous suspensions (0.4 mg/mL): ●, 1-C14/90°; ■, 1-C16/90°; ○, 1-C14/60°; and □, 1-C16/60°.

diffraction pattern (see Fig. 3). Thus, while the diffraction diagrams of the 1-C16 and 1-C18 complexes crystallized at 90° show the three major reflection peaks of the V-form (at 7.36, 13.1, and 20.1 2θ°) in the hydrated state, no distinct diffraction lines were observed for their 60° counterparts. These data confirmed the findings of Stute and Konieczny-Janda[15].

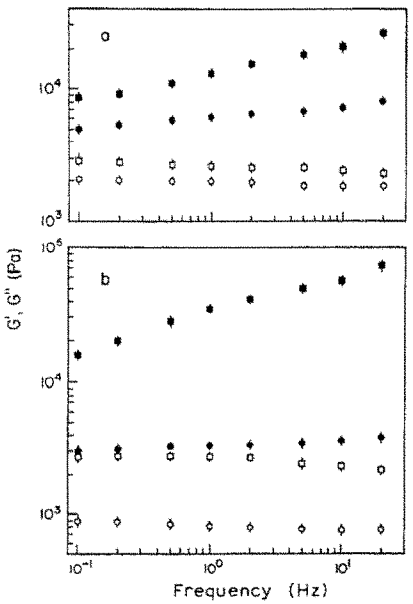

Fig. 5. Frequency dependence, mechanical spectra (●,■ G′ and ○,□ G″) of (a) amylose–monopalmitin and (b) amylose–monomyristin aqueous dispersions (10% w/v): squares, 60°-complexes; circles, 90°-complexes.

Differences in density and viscoelastic properties between aqueous suspensions of the structural forms I and II of amylose–monoglyceride complexes were also detected. Complexes of 1-C14 and 1-C16, crystallized at 90°, were more dense than those at 60°, as evidenced by the turbidity data of Fig. 4. These results suggested that the supermolecular structure of the 90° complex has a more compact organization than form I.

The mechanical spectra of aqueous dispersions for all complexes showed a slight frequency-dependence of both storage and loss moduli (G′,G″), typical of an elastic material rather than a viscoelastic solution (see Fig. 5). Dynamic rheological measurements of these samples were carried out in the linear viscoelastic region, where stress is proportional to strain. Clearly, the high-temperature complexes (form II) exhibited much lower values for G′ than those of form I for dispersions of equal solids content. In view of the observation that G′ increases with the volume fraction of the dispersed phase, the observed diferences in moduli between I and II could reflect merely differences in the respective volume fractions of the dispersed solids. Samples of a more compact supermolecular structure (*e.g.*, form II) are expected to occupy a much smaller volume fraction and thereby exhibit lower G′ values.

Preliminary crystallization experiments of amylose involving monostearin as the complexing agent have shown that forms I and II can be obtained as pure preparations (free from each other, as assessed by d.s.c. analysis) when complexation is carried out at either 60 or 90°, respectively. Because of their structural homogeneity, these samples were chosen for structural analysis studies by enzyme etching–gel permeation chromatography. The d.s.c. thermal curves of these complexes are given in Fig. 6. Hydrolytic action of α-amylase is expected to occur more rapidly in the disordered areas, whereas the ordered-chain domains would be more resistant[11]. Hence, chromatography of the residual amylodextrin fragments,

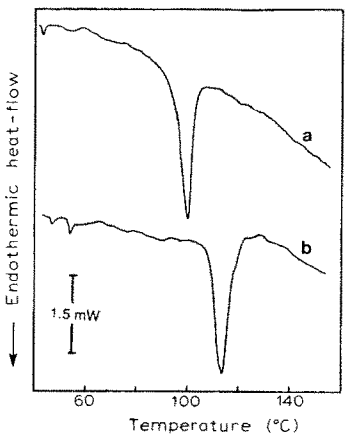

Fig. 6. D.s.c. thermal curves of amylose–monostearin complexes (20% w/w in H_2O) formed at (a) 60° and (b) 90°. Weight (mg) of complex from top to bottom: 1.95, 2.06.

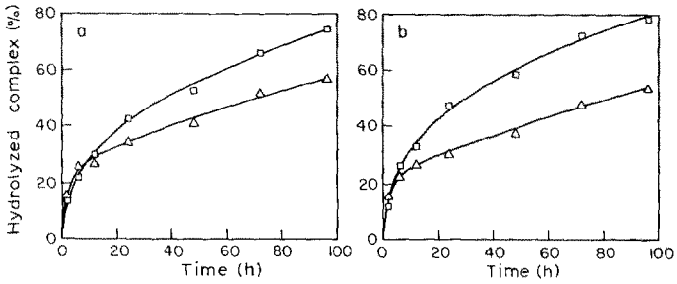

Fig. 7. Enzymic hydrolysis of amylose–monostearin complexes formed at (a) 60° and (b) 90° by *B. subtilis* (△) and porcine pancreatic (□) α-amylases.

following enzyme digestion in a heterogeneous reaction-mixture, can provide information on size distribution of the ordered-chain segments. Preliminary studies with BSA and PPA, using the experimental protocol of Jane and Robyt[11], indicated that long digestion periods were required to achieve a substantial degree of hydrolysis. Using their terminology, hydrolysis proceeded at a greater rate during the first 10 conversion periods (one conversion period is the time to convert amylose completely into maltodextrin products under identical incubation conditions; at a substrate to enzyme ratio of 20mg/IU, this time was ~2 h, presumably reflecting the digestion of the more-amorphous parts of the complexes (see Fig. 7). Thereafter, the residual amylodextrin fragments became less accessible to enzymic attack. The two-stage hydrolysis pattern is analogous to that observed with granular starch treated with mineral acids at temperatures below the gelatinization temperature[28,29]. During the second stage of hydrolysis, PPA caused, after a certain incuba-

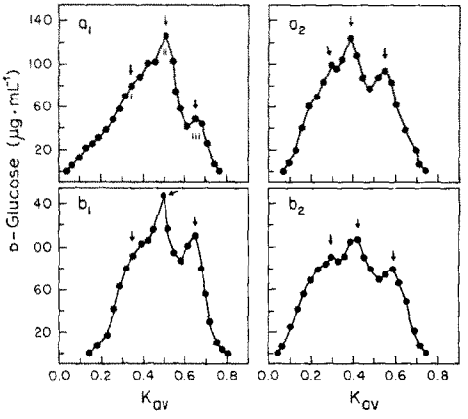

Fig. 8. Chromatographic profiles of resistant amylodextrin fragments, following α-amylase digestion of amylose–monostearin complexes for 48 h (20 mg of complex/IU) with *B. subtilis* (a_1, a_2) or porcine pancreatic (b_1, b_2) α-amylases, on a column (2.6 × 90 cm) of Sephacryl S-200 eluted with 2:3 (v/v) Me_2SO–water at a flow rate of 0.4 mL/min at 22°: a_1, b_1, 1-C18/60° complex; a_2, b_2, 1-C18/90° complex.

TABLE II

DEGREE OF POLYMERIZATION OF RESISTANT FRAGMENTS OF AMYLOSE-MONOSTEARIN COMPLEXES HYDROLYZED BY *B. subtilis* (BSA) AND PORCINE-PANCREATIC (PPA) α-AMYLASES

Complex/ crystallization temperature (°C)	*Enzyme*	*Degree of hydrolysis (%)*	*Degree of polymerization ($\overline{d.p.}$)*[a]		
			(i)	*(ii)*	*(iii)*
1-C18/60	BSA	41	107 sh[b]	80	50
	PPA	52	99 sh[b]	76	49
1-C18/90	BSA	38	147	100	60
	PPA	58	147	108	60

[a]The $\overline{d.p.}$ peak fraction values of i, ii, and iii chains, as designated by the arrows in the chromatograms of Fig. 8, were calculated using the calibration equation $\ln \overline{d.p.} = 5.873 - 3.055\ K_{av}$. Enzymic digestion with α-amylases for 48 h (20 mg of complex/IU), and chromatography on a column (2.6 × 90 cm) of Sephacryl S-200 eluted with 2:3 (v/v) Me_2SO–distilled water at a flow rate of 0.4 mL.min^{-1} at 22°. [b]sh, shoulder.

tion period, more extensive degradation than BSA for all samples. This difference may be due to the different requirements of the two enzymes for the number of binding subsites; 5 for PPA (ref. 30) and 9 for BSA (ref. 31). As a result, the BSA may leave a greater number of undigested fragments, interconnected with short, amorphous chain-segments. Interestingly, similar degradation kinetics were observed for the 60 and 90° complexes with each enzyme, despite the apparent differences in thermal stability and supermolecular organization.

In view of the biphasic hydrolysis profiles, it was decided to use the 48-h resistant amylodextrin fractions for gel filtration. The Sephacryl S-200 chromatograms of the ethanol-precipitated products revealed mainly three peaks of eluted material, as shown by the arrows in Fig. 8. The calculated peak d.p. values of these fractions for all four enzyme digests are summarized in Table II. It is of interest further to note that gel chromatography of the 96-h enzyme-treated complexes (data not shown), although their profiles were less defined than those of the 48-h, showed that K_{av} of fractions i, ii, and iii remained unchanged. These results would, therefore, imply that, even after extensive enzyme hydrolysis, in a heterogeneous reaction-mixture, the resistant amylodextrin has the initial chain-segment distribution for the ordered regions. With respect to complexes I and II, there were differences in the peak values of chains i, ii, and iii (see Table II); the 90° complex had chains of larger size. Nevertheless, it must be noted that, as between complexes I and II, all chromatograms had extensive overlapping zones for eluted carbohydrate material (see Fig. 8).

DISCUSSION

In considering thermally induced transitions of polymers in the presence of solvents, it must be remembered that the dynamic character of a polymeric

structure is dependent on the segmental mobility of the constituting chains. In fact, two important transitions are defined by increases in the segmental mobility: (*a*) glass–rubber transition at T_g, and (*b*) melting at T_m. The former is perhaps the most important property of any polymer in controlling its physical properties[32]. Below the T_g, the material is in its hard glassy state, where molecular motions are significantly restricted, whereas above T_g, the material is in its soft rubbery state. As a result, increased segmental motion in the amorphous domains above T_g allows structural transformations to occur, including increased chain-packing, crystallization, and annealing. Furthermore, of primary interest in the processing and functionality of polymeric materials is the need to know the responses of their supermolecular structure to solvents. For example, for semicrystalline starch-based systems in aqueous environments, the critical role of water for such processes as annealing, melting, and crystallization has been recently reviewed by Slade and Levine[33], and it can be best understood by taking into account both thermodynamic and kinetic contributions[17,18,20–22,23]. Water present in the amorphous phase acts as a plasticizer, thereby lowering its effective T_g (see refs. 20, 21, and 33). The T_g depression arises from a "lubricating" effect, leading to enhanced mobility of the amorphous chain-segments. Furthermore, the equilibrium melting point of the crystallites, T_m°, is depressed to a new value T_m if the amorphous phase contains water[18,20]. The latter is a thermodynamic effect due to polymer–diluent interactions and is described by the Flory–Huggins equation, assuming equilibrium conditions[34]. The importance of recognizing the depression of both T_g and T_m by water is clear when it is considered that such processes as annealing and crystallization can only occur between T_g and T_m, and that the kinetics of these phenomena are affected differently within the T_g–T_m temperature-region[20,21,33,35]. Similarly, recrystallization during d.s.c. heating can proceed only after exceeding the corresponding T_g of the respective system.

On analyzing various literature reports on amylose–lipid interactions, it was rather surprising to find how little attention has been paid to consideration of the supermolecular organization of the complexes. Thus, despite detailed comprehension of chain conformation and unit-cell dimensions[1–4,6–9], an understanding of the structural variables that contribute to, and control, the properties of the complexes has proved elusive. The main reason for the lack of progress in this area has been the difficulty in characterizing and quantifying such morphological variables as size, shape, and relative extent of fringing or folding for the ordered regions, and the true nature of the disordered material. As would be expected, these variables govern a wide variety of thermodynamic, spectral, and mechanical properties of these materials. In the following discussion, an attempt is made to provide some explanations of a number of physical and thermal properties of amylose–lipid complexes in terms of a working model for their supermolecular structure.

The results of the present study and other calorimetric reports[15,19] have shown that two thermally distinct, structural forms (I and II) of amylose–lipid complexes

exist, depending on the crystallization conditions (temperature, type of ligand, *etc.*). The differences in T_m between them (see Table I and Fig. 1) could be easily attributed to differences in size or perfection, or both, of their crystallites. In fact, melting data for synthetic linear polymers crystallized from dilute solution indicate that T_m is related to lamellar thickness[21,36]; *i.e.*, small or poor crystals, or both, grown under high supercooling conditions melt at much lower temperatures than larger crystals of higher perfection formed under low supercooling. However, in view of the X-ray diffraction data (see Fig. 3 and Table I), this possibility seems unlikely, because only form II shows clear evidence for the presence of well developed crystalline regions.

In contrast, the data for form I are indicative of a supermolecular organization of helices, with little crystallographic register. In this context, the observed density differences between I and II for both 1-C14 and 1-C16 (see Fig. 4) can also be explained on considering the marked difference in density between a true crystalline state and randomly distributed helical-chain segments. This reinforces the idea that only form II has well defined crystallites in its structure. The rheological data on the aqueous dispersions of the two complexes (see Fig. 5) are also consistent with such a view. In considering the volume fraction of the viscoelastic parameters (G',G''), at sufficiently low stresses to maintain linear viscoelasticity for the dispersed system, the more-dense 90° complexes did show lower storage and loss moduli (*i.e.*, occupy, a smaller volume fraction) than their 60° counterparts at an equal solids level. As to the size distribution of chain segments constituting the ordered regions, the chromatographic profiles of Fig. 8 (see also Table II) revealed minor differences between I and II; the 90° complex had larger peak d.p. values. Nevertheless, because most of the eluted material in both cases was of comparable size (see Fig. 8), the lack of V-type crystal structure of form I cannot be explained if a two-phase model is assumed for both complexes. Assuming 6 residues per helical turn, and leaving the required number of binding subsite residues on both sites of the lamellae, the d.p. of the central peak in the chromatograms (see fraction ii, Table II) of the 90° complexes corresponds to lamellar thicknesses of ~11 nm (BSA) and~13 nm (PPA). These values agree well with data obtained from X-ray crystallography[3,4,7], electron microscopy[3,4], and structural analysis by enzymic means[11]. According to the work of Jane and Robyt[11], fraction iii could originate from resistant amylodextrin fragments of retrograded amylose-chain segments.

The question then arises as to what are forms I and II, and what might be the thermodynamic and kinetic argumens for their existence, and for their transformation from one into the other? Form II is relatively easy to account for, as all of the experimental evidence presented herein points to the presence of crystallites embedded in, and molecularly continuous with, disordered chain segments. Although the exact morphology is not yet clear, based on the preferred mode of polymer crystallization from dilute solution[36] and on electron and X-ray diffraction studies on single amylose-V crystals[3,4,10], a lamellar organization would be the most

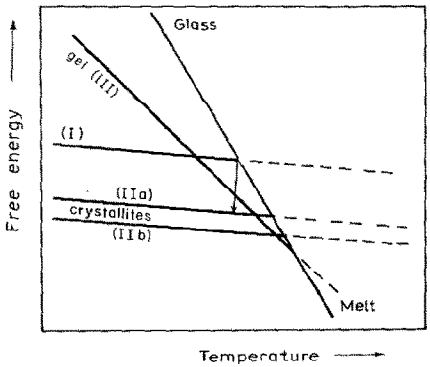

Fig. 9. Generalized schematic diagram of the free enthalpy of various structural forms of amylose. Forms I and II (complex) and III (gel) correspond to the transitions designated with the same notation in the thermal curves of Fig. 2. The straight lines are plots of free energy against temperature for each particular structural form.

likely structure. For form I, we propose that its structure has a much lower degree of localization of order, in which no distinct crystallites exist, but in which individual helical segments, not present in crystallographic register with one another, are randomly distributed throughout the material. Such a structure would thus have an internal energy and entropy lying intermediate between those of the liquid and the classical crystalline state. The fact that the calorimetric enthalpy values (ΔH_{cal}) associated with the order → disorder transition of forms I and II are of similar magnitude (see Table I) is fully consistent with this suggestion. On the basis of the fundamental relationship $\Delta H_{cal} - T\Delta S_{cal} = \Delta G = 0$ at T_m (*i.e.*, $T_m = \Delta H_{cal}/\Delta S_{cal}$), form I (of lower T_m) should have a conformational entropy higher than that of form II.

Accordingly, a generalized free-energy diagram of the two structural forms is illustrated in Fig. 9. The straight lines represent plots of free energy against temperature for forms I and II; their melting points are at the intersection of the respective F–T lines and the liquid free-energy line. The free energy relations shown in Fig. 9 can offer an explanation for the transformation of I → II which occurs after partial melting of form I (see Fig. 2b). This process (shown by the arrow in Fig. 9) is a conventional crystal-growth mechanism, involving the formation of crystallites by packing many helical-chain segments into crystallographic register; it should be noted that form II has much lower internal energy and entropy than form I. However, in order to form separate crystallites by alignment of neighboring helical regions considerable chain mobility must first be acquired. This condition appears to be satisfied only upon partial melting of structure I (see Fig. 2b and ref. 17). It must be noted that there is not any specific need for nucleation, as the unmelted helical structural motifs remaining can act as nuclei. The free-energy lines of IIa and IIb (corresponding to the melting transitions of Fig. 2) are drawn in order to indicate several metastable crystalline structures arising from a

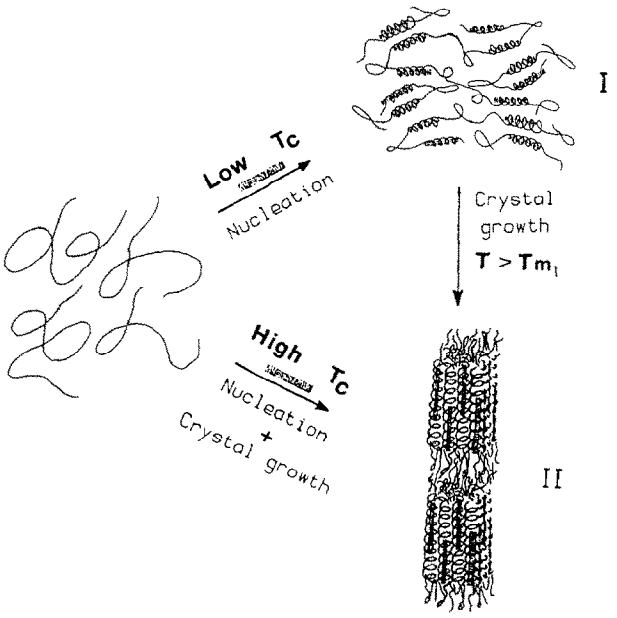

Fig. 10. Generalized mechanism for amylose–lipid complex-formation from dilute solutions which can account for the properties and postulated morphological features of Forms I and II.

progressive development of larger and more-perfect crystallites upon annealing. Finally, the free-energy line of the amylose gel structure, III (see Fig. 2c,d) is also presented in Fig. 9. The difference in the slope of this line is due to the following two reasons: (*a*) the internal energy and entropy of the amylose-gel network (non-retrograded state with little crystalline packing of chain duplexes) most likely lie in between the liquid and form I, and (*b*) the melting point of the gel is well above those of forms I and II, as shown in Fig. 2c,d; *i.e.*, the gel F–T line must cross the liquid free-energy line at a higher temperature. It is also possible to capture an amylose "melt" in a glassy state, if the system is quenched-cooled to a temperature below its effective T_g, the latter being dependent on the moisture content of the amorphous phase.

CONCLUSIONS

The reported structure–property relationships for amylose-V complexes as revealed by a variety of analytical approaches suggest the need for expansion of the conclusions drawn from our earlier studies over a narrower range of experimental conditions and based solely on calorimetric measurements[17,18]. As such, the arguments presented herein are intended to show that the experimental evidence on multiple melting phenomena of amylose–lipid complexes and their physicochemical properties can be explained if it is postulated that forms I and II

are two separate thermodynamic states. A simplified mechanism for complex-formation from dilute solutions which can account for the properties, morphological features, and transformations as already discussed is depicted in Fig. 10. According to this scheme, at low temperatures (T_c), formation of complex I is the favored process. Although this form is metastable in character, its existence is determined mainly by kinetics. In the presence of good complexing agents, and at low T_c, the nucleation rate is high, thereby causing rapid "freezing" of helical-chain segments with very little crystallographic register (form I) throughout the structure. As such, interhelical amorphous chain regions would be under considerable strain and it is likely that they would exhibit an elevated T_g, very close to T_{mI} of the helices. This implies that high energy-barriers between the two forms exist and, therefore, that unless the system is partially melted, it would remain practically unchanged at $T < T_{mI}$. On the other hand, at high T_c, the nucleation density would be much lower, and thus complex-formation is allowed to progress as a conventional crystallization process, thereby leading to a partially crystalline structure.

ACNOWLEDGMENTS

The support of a research operating grant from the Natural Sciences and Engineering Research Council of Canada is gratefully acknowledged. The authors also acknowledge the technical assistance of G. Steidl. We are grateful to Henry Zobel for reviewing this manuscript.

REFERENCES

1 R. E. RUNDLE AND F. C. EDWARDS, *J. Am. Chem. Soc.*, 65 (1943) 2200–2203.
2 F. F. MIKUS, R. M. HIXON, AND R. E. RUNDLE, *J. Am. Chem. Soc.*, 68 (1946) 1115–1123.
3 R. S. J. MANLEY, *J. Polym. Sci., Part A*, 2 (1964) 4503–4515.
4 Y. YAMASHITA, *J. Polym. Sci., Part A*, 3 (1965) 3521–3260.
5 K. TAKEO, A. TOKUMURA, AND T. KUGE, *Staerke*, 25 (1973) 357–362.
6 D. FRENCH, A. O. PULLEY, AND W. J. WHELAN, *Staerke*, 15 (1963) 349–354.
7 B. ZASLOW, *Biopolymers*, 1 (1963) 165–169.
8 T. D. SIMPSON, F. R. DINTZIS, AND N. W. TAYLOR, *Biopolymers*, 11 (1972) 2591–2600.
9 Y. YAMASHITA AND K. MONOBE, *J. Polym. Sci., Part A-2*, 9 (1971) 1471–1481.
10 A. BULEON, F. DUPRAT, F. P. BOOY, AND A. CHANZY, *Carbohydr. Polym.*, 4 (1984) 161–173.
11 J. L. JANE AND J. F. ROBYT, *Carbohydr. Res.*, 132 (1984) 105–118.
12 M. KUGIMIYA, J. W. DONOVAN, AND R. Y. WONG, *Staerke*, 32 (1980) 265–270.
13 P. V. BULPIN, E. J. WELSH, AND E. R. MORRIS, *Staerke*, 34 (1982) 335–339.
14 A. C. ELIASON AND N. J. KROG, *Cereal Sci.*, 2 (1985) 239–248.
15 V. R. STUTE AND G. KONIECZNY-JANDA, *Staerke*, 35 (1983) 340–347.
16 M. KOWBLANSKY, *Macromolecules*, 18 (1985) 1776–1779.
17 C. G. BILIADERIS, C. M. PAGE, L. SLADE, AND R. R. SIRETT, *Carbohydr. Polym.*, 5 (1985) 367–389.
18 C. G. BILIADERIS, C. M. PAGE, AND T. J. MAURICE, *Carbohydr. Polym.*, 6 (1986) 269–288.
19 C. G. BILIADERIS, C. M. PAGE, AND T. J. MAURICE, *Food Chem.*, 22 (1986) 279–295.
20 C. G. BILIADERIS, C. M. PAGE, T. J. MAURICE, AND B. O. JULIANO, *J. Agric. Food Chem.*, 34 (1986) 6–14.
21 L. SLADE AND H. LEVINE, *Proc. Conf. N. Am. Thermal Anal. Soc., 13th*, University of Pennsylvania, 1984, p. 64.
22 T. J. MAURICE, L. SLADE, R. R. SIRETT, AND C. M. PAGE, in D. SIMATOS AND J. L. MULTON (Eds.), *Properties of Water in Food*, Martinus Nijhoff, Dordrecht, Netherlands, 1985, pp. 211–227.

23 B. WUNDERLICH, *Macromolecular Physics*, Vol. 3, Academic Press, New York, 1980.
24 J. M. G. COWIE AND C. T. GREENWOOD, *J. Chem. Soc.*, (1957) 2862–2866.
25 N. NELSON, *J. Biol. Chem.*, 153 (1944) 375–380.
26 N. KROG, *Staerke*, 23 (1971) 206–210.
27 C. G. BILIADERIS, D. R. GRANT, AND J. R. VOSE, *Cereal Chem.*, 58 (1981) 496–502.
28 J. P. ROBIN, C. MERCIER, R. CHARBONNIERE, AND A. GUILBOT, *Cereal Chem.*, 51 (1974) 389–406.
29 C. G. BILIADERIS, D. R. GRANT, AND J. R. VOSE, *Cereal Chem.*, 58 (1981) 502–507.
30 J. F. ROBYT AND D. FRENCH, *Arch. Biochem. Biophys.*, 122 (1967) 8–16.
31 J. F. ROBYT AND D. FRENCH, *Arch. Biochem. Biophys.*, 100 (1963) 451–467.
32 A. EISENBERG, in M. J. E. MARK, A. EISENBERG, W. W. GRAESSLEY, L. MANDELKERN, AND J. L. KOENIG (Eds.), *Physical Properties of Polymers*, American Chemical Society, Washington, D.C., 1984, pp. 55–95.
33 L. SLADE AND H. LEVINE, in S. S. STIVALA, V. CRESCENZI, AND I. C. M. DEA (Eds.), *Industrial Polysaccharides*, Gordon and Breach Science Publishers, New York, 1987, pp. 387–430.
34 P. J. FLORY, *Principles of Polymer Chemistry*, Cornell University Press, Ithaca, N.Y., 1953.
35 H. LEVINE AND L. SLADE, *Carbohydr. Polym.*, 6 (1986) 213–244.
36 B. WUNDERLICH, *Macromolecular Physics*, Vol. 2, Academic Press, New York, 1976.